

# PREPARATION OF COPPER-SUPPORTED MESOPOROUS CARBON/EPOXY COMPOSITES AND THEIR THERMAL PROPERTIES

GUN-YOUNG HEO, SOO-JIN PARK\*

Department of Chemistry, Inha University, 253, Nam-gu, Incheon 402-751, Korea

\* Corresponding author(sjpark@inha.ac.kr)

**Keywords:** *Copper-supported mesoporous carbon, XRD, BET surface area, pore volume, thermal conductivity*

## Abstract

In this work, the copper-supported mesoporous carbon (Cu-CMK-3) materials were prepared by impregnating mesoporous carbon (CMK-3) with copper (II) acetylacetonate. And the effects of the supported-copper on thermal properties of the epoxy/Cu-CMK-3 were investigated by X-ray diffraction (XRD), Brunauer–Emmett–Teller (BET) and thermal conductivity. As experimental results, the supported-copper on CMK-3 was confirmed from the decreasing of the BET surface area and the pore volume. The curing reactivities of DGEBF/Cu-CMK-3 were decreased with the supported-copper. Also, the initial decomposition temperature (IDT) of DGEBF/Cu-CMK-3 was higher than that of DGEBF/CMK-3. This could be interpreted in terms of high thermal dissipation properties resulting in the Cu existing in the pore volume. Thermal conductivity of DGEBF /Cu-CMK-3 was considerably increased with usage of the copper-supported mesoporous carbon.

## Introduction

Epoxy resins cannot be used alone for high performance applications because they have limited properties such as electrical and thermal conductivities. Therefore, epoxy/filler composites are often applied in order to overcome the problems. One of the widely used reinforcing filler is carbon materials.<sup>1-5</sup>

Mesoporous carbon materials are excellent materials with high specific surface area, low density, low dielectric constant and low thermal conductivity. Therefore, they have many potential applications in thermal, acoustic, electronic and catalytic fields, especially in thermal insulation.<sup>6-10</sup>

Meanwhile, metal-supported carbon catalysts are industrially important and are used for fine chemical and alternative fuel industry. In particular, their catalytic decomposition to CO and hydrogen is a considerable interest in the application of methanol as an alternative ecological fuel. Some copper containing carbon materials appear to be promising catalysts for this purpose.<sup>11-15</sup>

Copper-supported mesoporous carbon materials have many unique properties. The supported copper on carbon materials enables to resist chemical erosion, enhances the stability of the carbon materials, and improves the composite properties, such as higher electrical conductivity, magnetism and good adhesion. Generally, the impregnating method has been widely used for metal supporting on carbon materials. Mesoporous carbon materials have also been supported with Cu, with applications in the field of capacitor, catalyst, and electromagnetic shielding.<sup>15-17</sup>

In this work, the copper-supported mesoporous carbon (Cu-CMK-3) materials were prepared by impregnating mesoporous carbon (CMK-3) with copper (II) acetylacetonate. The goal of this work was to determine the effects of supported-copper on thermal properties of epoxy/Cu-CMK-3.

## Experimental

### Materials

Epoxy resin used for this study was diglycidylether of bisphenol F (DGEBF supplied from Japan Epoxy Resins. Co. Ltd.). The epoxide equivalent weight of the DGEBF was 170 g/eq. and the density was 1.16 g·cm<sup>-3</sup> at 25 °C. The diaminodiphenylmethane (DDM) as a curing agent was purchased from Aldrich Chem. Co. (Milwaukee, WI). The chemical structures of DGEBF and diamino- diphenylmethane

were shown in Fig. 1 (a) and (b), respectively.

All organic starting materials used for the synthesis of the CMK-3, such as P123 (PEO<sub>20</sub>PPO<sub>70</sub>PEO<sub>20</sub>), tetraethyl orthosilicate (TEOS), and sucrose (C<sub>12</sub>H<sub>22</sub>O<sub>11</sub>) were purchased from the Aldrich Chem. Co. (Milwaukee, WI). Other solvents were used as received and all reagents were used without further purification.

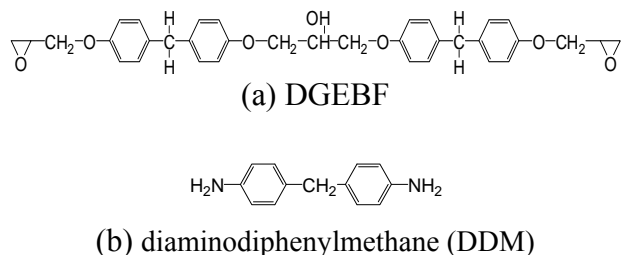
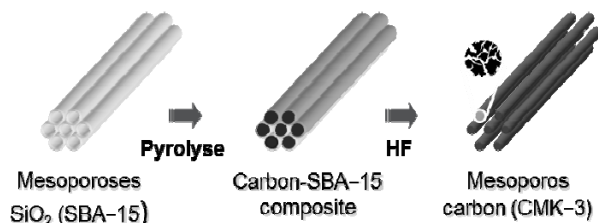


**Fig. 1.** Chemical structures.

### Preparations of CMK-3 and Cu-CMK-3

The CMK-3 was synthesized by conventional templating method using SBA-15, following the method by Sakamoto and co-workers.<sup>18</sup> The synthesis route for CMK-3 was depicted in Scheme 1.



**Scheme 1.** Synthesis route for CMK-3.

Copper-supported mesoporous carbon (Cu-CMK-3) materials were prepared by impregnating mesoporous carbon (CMK-3) with copper (II) acetylacetonate. Here, the added Cu (II) content for loading was 10phr. 0.10 g of Cu (II) acetylacetonate were dissolved in 20 ml of chloroform and 1 g of CMK-3 was added. The suspension was stirred for 4 h at room temperature and then the chloroform was evaporated by mild heating (80°C) of the sample. Subsequently, the product was washed with chloroform to remove excess copper acetate on the outer surface, filtered and dried.

### Preparations of specimens

To prepare the specimens, the DGEBF were degassed in vacuum oven at 100°C for 2 h. The CMK-3 or Cu-CMK-3 1phr as the filler was added to the DGEBF with continuous stirring until a homogeneous mixture was obtained. Then the DDM as the curing agent was added to the homogeneous mixture. The curing step was 110°C for 1 h, 140°C for 2 h, and 170°C for 1 h in a convection oven.

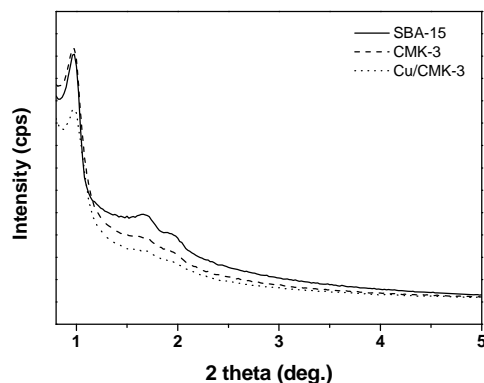
### Characterization and measurements

The structure of the samples was evaluated by powder X-ray diffraction (XRD) recorded on a Rigaku D/Max-III B system using CuKα radiation. Brunauer–Emmett–Teller (BET) surface area and pore diameters were determined by nitrogen adsorption/desorption isotherms at 77K using a static volumetric technique. Differential scanning calorimeter (Perkin-Elmer, model DSC 6) was used for monitoring of curing behaviors of the DGEBF/CMK-3 and DGEBF/Cu-CMK-3 at between room temperature and 200°C using a heating rate of 10 °C/min, under a nitrogen atmosphere. Thermal stabilities of the DGEBF/CMK-3 and DGEBF/Cu-CMK-3 were determined by thermogravimetric analysis (TGA). All TGA analyses were performed with a NETZSCH TGA 209 at heating rate 10°C/min from 30 to 850°C under the condition of nitrogen gas. Thermal conductivities of the DGEBF/CMK-3 and DGEBF/Cu-CMK-3 composites were measured using the thermal conductivity analyzer (LFA 447, NETZSCH). Each specimen was indented three times, and the mean values were used in this paper.

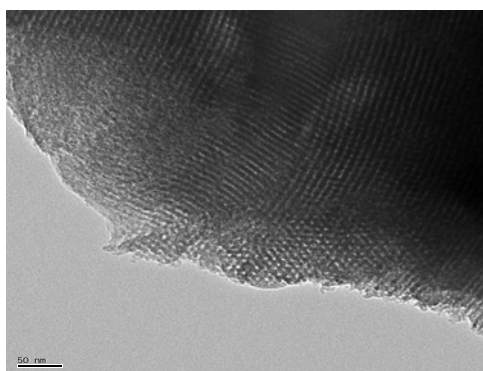
### Results and Discussion

Fig. 2 and Fig. 3 show X-ray diffraction (XRD) pattern and transmission electron microscope (TEM) image of the synthesized CMK-3, respectively. As shown in the Fig. 2, the intense peak at low angle can be attributed to the 100 reflection and two peaks at higher angles attributed to the 110 and 200 reflections. From these patterns, the CMK-3 gives typical XRD pattern of 2-d hexagonal (P6mm) structure.<sup>19</sup> The hexagonal pore structure is further confirmed by TEM observations. As shown in the Fig. 2, the framework hexagonal ordering of Cu-CMK-3 materials was basically retained after the

loading of Cu. This could be interpreted in terms of existence of the main diffraction peak (100). However, the intensity of (110), and (200) diffraction peaks was decreased with increasing the loading of Cu.



**Fig. 2.** Low angle XRD curves of the pure CMK-3 and Cu-CMK-3.



**Fig. 3.** TEM image of CMK-3.

The specific surface areas (SBET) of the pure CMK-3 and Cu-CMK-3 were calculated by the Brunauer–Emmett–Teller (BET) method. The results were summarized in Table 1.

**Table 1.** Textural Properties of the CMK-3.

	$S_{BET}^a$	$V_T^b$
CMK-3	891	1.13
Cu-CMK-3	565	0.81

<sup>a</sup> Specific surface area (m<sup>2</sup>/g), <sup>b</sup> Total pore volume (cm<sup>3</sup>/g)

As shown in the Table 1, the BET surface area and total pore volume of Cu-CMK-3 were considerably decreased with the added copper.

Fig. 4 shows the DSC thermograms of DGEBF/CMK-3 and DGEBF/Cu-CMK-3 with DDM.

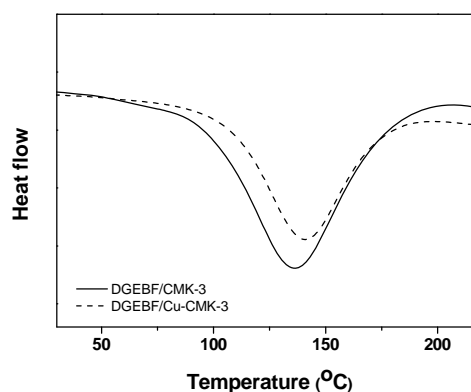


**Fig. 4.** DSC thermograms of DGEBF/CMK-3 and DGEBF/Cu-CMK-3.

As shown in Figure 4, the DSC thermograms of the DGEBF/CMK-3 and DGEBF/Cu-CMK-3 were very similar but the initial curing temperature of DGEBF/Cu-CMK-3 was higher than that of DGEBF/CMK-3. The maximum peak temperature showed at 136 °C and 141 °C, respectively.

The curing reactivity of DGEBF/CMK-3 and DGEBF/Cu-CMK-3 were characterized with the measurement of the conversion as a function of the temperature. The conversion was determined on the basis of the DSC thermograms and the following eq. (1):<sup>20</sup>

$$\text{Conversion } (\alpha_t) = \frac{\Delta H_t}{\Delta H_{Total}} \times 100 \quad (1)$$

where  $\alpha_t$  is the conversion at time (t),  $\Delta H_t$  is the accumulated heat released before time t, and  $\Delta H_{Total}$  is the total heat released at the end of the reaction.

Fig. 5 shows the conversion as a function of the curing temperature for of DGEBF/CMK-3 and DGEBF/Cu-CMK-3 obtained from the DSC thermograms. As shown in Fig. 5, it was clear that the conversions of DGEBF/Cu-CMK-3 move to high temperature with the adding of the CMK-3. This was due to the Cu that exists in CMK-3. The

ring opening reaction of epoxides was delayed by the Cu in pore of the CMK-3.

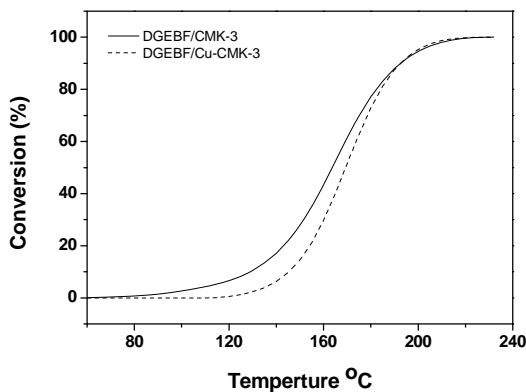


**Fig. 5.** Conversion of DGEBF/CMK-3 and DGEBF/Cu-CMK-3.

To investigate more detailed the effect of the Cu-CMK-3 on thermal properties, TGA thermograms were obtained with a thermal analyzer. Figure 6 shows the TGA thermograms of the pure DGEBF, DGEBF/CMK-3 and DGEBF/Cu-CMK-3. As shown in Figure 6, the initial decomposition temperature (IDT) of DGEBF/Cu-CMK-3 was higher than that of the DGEBF/CMK-3 but decomposition behaviors at between 360°C and 420°C was very similar. Also, the DGEBF/Cu-CMK-3 showed the highest amount of residue, resulting in the Cu in pore of the CMK-3. From these results, it was confirmed that the introduction of Cu proceeded well.

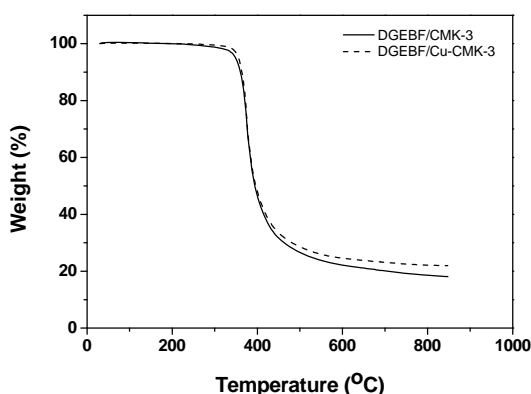


**Fig. 6.** TGA thermograms of DGEBF/CMK-3 and DGEBF/Cu-CMK-3.

Thermal conductivity of the cured specimens was measured by the Netzsch laser flash diffusivity system, LFA 447. The flash parameters used for this

experiment were a laser voltage of 270 V, 100% open filter.

The thermal conductivities of the DGEBF/pure CMK-3 and DGEBF/Cu-CMK-3 composites obtained from the Netzsch laser flash diffusivity system are indicated in Table 2

**Table 2.** Thermal conductivities of DGEBF/CMK-3 and DGEBF/Cu-CMK-3.

	Thermal Conductivity (W/(m·K))
DGEBF /CMK-3	0.24
DGEBF /Cu-CMK-3	0.32

As shown in Table 2, the thermal conductivity was increased with usage of the copper-supported mesoporous carbon. The low thermal conductivity of DGEBF/Cu-CMK-3 is because the thermal diffusion in the matrix resin is improved by the copper existing in the pore of CMK-3.

## Conclusions

Supported-copper on mesoporous carbon could be to decrease the curing reactivity of DGEBF but that had not a significant effect on the decomposition behaviors of the DGEBF except for the IDT. Also, thermal conductive property of DGEBF/mesoporous carbon could be improved by mixing the copper-supported mesoporous carbon (Cu-CMK-3). This was due to the facts that the supported copper has a relatively high dissipation property.

## References

- [1] M. M. Schwartz, "Composite Materials Handbook", 2nd ed., McGraw-Hill, New York, 1992.
- [2] C. A. May, "In Epoxy Resins: Chemistry and Technology", 2nd Ed.; Marcel Dekker: New York, 1988.
- [3] S. J. Park, K. M. Bae, and M. K. Seo "A study on rheological behavior of MWCNTs/epoxy composites", J. Ind. Eng. Chem., Vol. 16, No. 3, 337-339, 2010.
- [4] F. E. Tantawy, K. Kamada, and H. Ohnabe, "In situ network structure, electrical and thermal properties of conductive epoxy resin-carbon black composites for electrical heater

- applications”, *Mater. Lett.*, Vol 56, 112-126, 2002.
- [5] L. Guadagno, B. De Vivo, A. Di Bartolomeo, P. Lamberti, A. Sorrentino, V. Tucci, L. Vertuccio, and V. Vittoria, “Effect of functionalization on the thermo-mechanical and electrical behavior of multi-wall carbon nanotube/epoxy composites”, *Carbon*, Vol. 49, 1919-1930, 2011.
- [6] T. Kyotani, “Control of pore structure in carbon,” *Carbon*, Vol.38, 269-286, 2000.
- [7] X. Bo, J. Bai, L. Wang, and L. Guo, “In situ growth of copper sulfide nanoparticles on ordered mesoporous carbon and their application as nonenzymatic amperometric sensor of hydrogen peroxide” *Talanta*, Vol. 81(1-2), 339, 2010.
- [8] Y. Hou, L. Guo, and G. Wang, J. “Synthesis and electrochemical performance of ordered mesoporous carbons with different pore characteristics for electrocatalytic oxidation of hydroquinone” *Electroanal. Chem.*, Vol. 617, 211-217, 2008.
- [9] B. J. Kim, Y. S. Lee, and S. J. Park, “A study on the hydrogen storage capacity of Ni-plated porous carbon nanofibers”, *Int. J. Hydrogen Energy*, Vol. 33, 4112-4115, 2008.
- [10] B. Liu and S. Creager, “Silica-sol-templated mesoporous carbon as catalyst support for polymer electrolyte membrane fuel cell applications”, *Electrochim. Acta*, Vol. 55, 2721-2726, 2010.
- [11] Y. Li, D. Li, and G. Wang, “Methane decomposition to CO<sub>x</sub>-free hydrogen and nano-carbon material on group 8–10 base metal catalysts: A review”, *Catalysis Today*, Vol. 162(1): 1-48, 2011
- [12] S. K. Papageorgiou, E. P. Favvas, A. A. Sapalidis, G. E. Romanos, and F. K. Katsaros, “Facile synthesis of carbon supported copper nanoparticles from alginate precursor with controlled metal content and catalytic NO reduction properties”, *J. Hazard. Mater.*, Vol. 189(1-2): 384-390, 2011.
- [13] J. R. C. Salgado, F. Alcaide, G. Álvarez, L. Calvillo, M.J. Lázaro, and E. Pastor, “Pt–Ru electrocatalysts supported on ordered mesoporous carbon for direct methanol fuel cell” *J. Power Sources*, Vol. 95, 4022-4029, 2010.
- [14] L. Calvillo, V. Celorrio, R. Moliner, and M.J. Lázaro, “Influence of the support on the physicochemical properties of Pt electrocatalysts: Comparison of catalysts supported on different carbon materials”, *Mater. Chem. Physics*, Vol. 127, 335-341, 2011.
- [15] S. Tan, W. Zou, F. Jiang, S. Tan, Y. Liu, D. Yuan, “Facile fabrication of copper-supported ordered mesoporous carbon for antibacterial behavior” *Mater. Lett.*, Vol. 64, 2163-2166, 2010.
- [16] M. Yang and Q. Gao, “Copper oxide and ordered mesoporous carbon composite with high performance using as anode material for lithium-ion battery” *Microporous Mesoporous Mater.*, In Press,
- [17] L. J. Kennedy, A. G. Kumar, B. Ravindran and G. Sekaran, “Copper impregnated mesoporous activated carbon as a high efficient catalyst for the complete destruction of pathogens in water”, *Environ. Prog.*, Vol. 27, 40–50, 2008.
- [18] Y. Sakamoto, M. Kaneda, O. Terasaki, DY. Zhao, J. M. Kim, GH. Stucky, J. Shin, and R. Ryoo, “Direct imaging of the pores and cages of three-dimensional mesoporous materials”, *Nature*, Vol. 408: 449-453, 2000.
- [19] N. Gokulakrishnan, N. Kania, B. Léger, C. Lancelot, D. Grosso, E. Monflier, and A. Ponchel, “An ordered hydrophobic P6mm mesoporous carbon with graphitic pore walls and its application in aqueous catalysis”, *Carbon*, Vol. 49, 1290-1298, 2011.
- [20] G. Y. Heo and S. J. Park, “Effect of substituted Trifluoromethyl groups on thermal and mechanical properties of fluorine-containing epoxy resin”, *Macromol. Resear.*, Vol. 17, 870-873, 2009.